AEM
Journals.ASM.org

Actinobacterial Nitrate Reducers and Proteobacterial Denitrifiers Are Abundant in N_2O-Metabolizing Palsa Peat

Katharina Palmer and Marcus A. Horn

Department of Ecological Microbiology, University of Bayreuth, Bayreuth, Germany

Palsa peats are characterized by elevated, circular frost heaves (peat soil on top of a permanently frozen ice lens) and are strong to moderate sources or even temporary sinks for the greenhouse gas nitrous oxide (N_2O). Palsa peats are predicted to react sensitively to global warming. The acidic palsa peat Skalluvaara (approximate pH 4.4) is located in the discontinuous permafrost zone in northwestern Finnish Lapland. *In situ* N_2O fluxes were spatially variable, ranging from 0.01 to −0.02 μmol of N_2O m^{-2} h^{-1}. Fertilization with nitrate stimulated *in situ* N_2O emissions and N_2O production in anoxic microcosms without apparent delay. N_2O was subsequently consumed in microcosms. Maximal reaction velocities (v_{max}) of nitrate-dependent denitrification approximated 3 and 1 nmol of N_2O per h per gram (dry weight [g_{DW}]) in soil from 0 to 20 cm and below 20 cm of depth, respectively. v_{max} values of nitrite-dependent denitrification were 2- to 5-fold higher than the v_{max} nitrate-dependent denitrification, and v_{max} of N_2O consumption was 1- to 6-fold higher than that of nitrite-dependent denitrification, highlighting a high N_2O consumption potential. Up to 12 species-level operational taxonomic units (OTUs) of *narG*, *nirK* and *nirS*, and *nosZ* were retrieved. Detected OTUs suggested the presence of diverse uncultured soil denitrifiers and dissimilatory nitrate reducers, hitherto undetected species, as well as *Actino-*, *Alpha-*, and *Betaproteobacteria*. Copy numbers of *nirS* always outnumbered those of *nirK* by 2 orders of magnitude. Copy numbers of *nirS* tended to be higher, while copy numbers of *narG* and *nosZ* tended to be lower in 0- to 20-cm soil than in soil below 20 cm. The collective data suggest that (i) the source and sink functions of palsa peat soils for N_2O are associated with denitrification, (ii) actinobacterial nitrate reducers and *nirS*-type and *nosZ*-harboring proteobacterial denitrifiers are important players, and (iii) acidic soils like palsa peats represent reservoirs of diverse acid-tolerant denitrifiers associated with N_2O fluxes.

Permafrost systems in the Northern Hemisphere cover about 16% of the global soil surface area, store substantial amounts of carbon and nitrogen, and are therefore important players in the global carbon and nitrogen cycles (54, 67). Palsas are elevations of peat soil above the ground level due to uplifting of peat layers by a frozen ice lens and are mainly encountered in the discontinuous permafrost zone (63). Palsa peatlands are widely distributed in the Arctic, including Canada, Norway, Sweden, Iceland, Russia (Siberia), the United States (Alaska), and Finland (62, 75). Palsa development is affected by various environmental factors, such as wind erosion, vegetation cover, snow cover, and ground water table depth (63). High-latitude peatlands have been intensively studied with respect to their capacity to emit methane due to the large amount of stored carbon in peat soils, but nitrous oxide (N_2O) emissions from permafrost regions were generally considered to be insignificant (12, 58, 66). However, recent studies document significant but variable N_2O emissions from permafrost systems including palsas (17, 45, 58). N_2O is the major ozone-depleting substance in the atmosphere (57), and such N_2O emissions might well impact climate change since the global warming potential of N_2O is approximately 300 times that of CO_2 (20). Palsa peats are predicted to be strongly affected by global warming (2, 21, 63). Increasing temperatures are generally anticipated to reduce the water table in northern peatlands and to increase the amount of CO_2, CH_4, and N_2O released from peatland soils (2, 44, 45).

N_2O is produced during nitrification, denitrification, or chemical processes in soils (8, 13). N_2O is an intermediate during denitrification, and denitrification is considered to be the main source of and hypothesized to represent a sink for N_2O in water-saturated soils including peatlands and is an essential part of the nitrogen cycle (11, 13, 48). Nitrate or nitrite is sequentially reduced via nitric oxide (NO) and N_2O to dinitrogen (N_2) during denitrification (76). Such reductions are catalyzed by a set of oxidoreductases, namely, nitrate reductases (encoded by *narG* and *napA*), nitrite reductases (encoded by *nirK* and *nirS*), NO reductases (encoded by *norBC* or *norZ*), and N_2O reductases (encoded by *nosZ*) (76, 77). Nitrate reductases likewise catalyze nitrate reduction by nondenitrifying dissimilatory nitrate reducers (52). N_2O and N_2 can be released into the atmosphere, and the ratio of N_2O to N_2 is determined by *in situ* parameters such as pH, temperature, and oxygen content, as well as nitrate/nitrite and electron donor availability (69). pH is one of the main factors impacting denitrification; low pH decreases overall denitrification rates and increases the product ratio of N_2O to N_2 (64). Although pristine northern peatlands including palsas are characterized by low pH and although evidence is accumulating that northern peatlands emit N_2O, palsas might represent temporary sinks for N_2O; however, microbial communities involved in N_2O turnover and N-cycling in northern peatlands are largely unknown to date (24, 45, 47, 48).

There is a particularly high deficit of information on N_2O fluxes from palsa peats, the underlying processes, their regulation, and the associated acid-tolerant microbial communities. Thus, the main objectives of this study were to (i) assess *in situ* N_2O

Received 10 March 2012 **Accepted** 23 May 2012

Published ahead of print 1 June 2012

Address correspondence to Marcus A. Horn, marcus.horn@uni-bayreuth.de.

Supplemental material for this article may be found at http://aem.asm.org/.

doi:10.1128/AEM.00810-12

TABLE 1 Soil parameters of Skalluvaara palsa peat[a]

Soil layer or source	pH	Moisture content (%)	NO_3^- concn		NO_2^- concn		NH_4^+ concn		Total C ($g\ kg_{DW}^{-1}$)	DOC[b] ($mg\ liter^{-1}$)	Total N ($g\ kg_{DW}^{-1}$)	C/N[c]
			μM	μmol g_{DW}^{-1}	μM	μmol g_{DW}^{-1}	μM	μmol g_{DW}^{-1}				
0–20 cm	4.6	73 ± 0.2	<26	<0.07	<60	<0.16	125.0	6.0	505	217	18	29
Below 20 cm	4.2	76 ± 0.2	<25	<0.08	<57	<0.18	106.0	6.0	501	156	19	26
Stream water	6.7	NA[d]	<4.7	NA	<11	NA	<1.4	NA	NA	7.2	NA	NA

[a] All values for 0- to 20-cm soil and below-20-cm soil, with the exception of moisture content, were determined from pooled soil samples of four replicate palsas.
[b] DOC, dissolved organic carbon.
[c] Carbon-to-nitrogen ratio.
[d] NA, not applicable.

fluxes and *in situ* N_2O emission capacities of palsa peat soil, (ii) determine N_2O production and consumption potentials of palsa peat denitrifiers in microcosms, (iii) derive apparent Michaelis-Menten-like kinetic parameters, and (iv) characterize the denitrifier community composition and abundance in palsa peat soil by bar-coded amplicon pyrosequencing coupled to quantitative PCR of multiple denitrification or nitrate reduction associated genes.

MATERIALS AND METHODS

Sampling site. The palsa peat Skalluvaara is located in northwestern Finnish Lapland (69°49′13″N, 27°9′47″E) at an elevation of 280 m above sea level, 6 km northwest of Stuorra Skállovárri (Great Skalluvaara, 408 m above sea level). The mean annual air temperature is −1.6 ± 1.2°C, the mean air temperature in July is 12.9°C (range, 2.9 to 26.9°C), and the mean monthly precipitation approximates 34.6 ± 6.7 mm (average of years 1962 to 2008, measured at Kevo research station). Palsas are elevated about 20 to 100 cm above the peat surface. Plant cover of palsas and surrounding peat soil consists mainly of *Rubus chamaemorus*, *Vaccinium myrtillus*, *Vaccinium vitis-idea*, *Vaccinium uliginosum*, *Empetrum nigrum*, *Rhododendron tomentosum*, *Cornus suecica*, *Sphagnum fallax*, *Sphagnum riparium*, *Betula pubescens* subsp. *czerepanovii*, and *Betula nana*. Soil temperature was 12°C in surface soil (16 July 2010), and palsas were frozen at 30 to 35 cm below palsa surface. Soil samples from layers at 0 to 20 cm and from 20 cm to the top of the frozen core (i.e., below 20 cm) were collected from four different vegetated palsas in July 2010. Samples were transported on ice to the laboratory and stored at 4°C for microcosm analyses or at −80°C for nucleic acid extractions within 1 h after sampling. Microcosm experiments were conducted within 2 weeks after sampling.

Assessment of *in situ* gas emissions. *In situ* gas emissions of unfertilized palsa peat and palsas fertilized with either nitrate or ammonium were determined in closed Plexiglas chambers. Two liters of water from a nearby stream that was supplemented with 20 mM sodium nitrate or 20 mM ammonium chloride was distributed homogeneously on top of approximately 0.25 m^2 of the soil in four replicates. Soil that received unsupplemented stream water served as a control. Stream water nitrate, nitrate, ammonium, and dissolved organic carbon (DOC) concentrations were negligible (Table 1). Plexiglas chambers were placed on metal collars, which had been inserted into the soil for a few centimeters (31). The transition between Plexiglas chamber and metal collar was sealed with a rubber band to avoid exchange of gases from the chamber with the surrounding air. Gas samples (5 ml per sampling time point) were taken from gas outlets and injected into gas-tight Exetainers (Labco Limited, High Wycombe, United Kingdom) immediately after fertilization and after 0.5, 1, and 3 h.

Assessment of denitrification in soil microcosms. Soil was homogenized and mixed prior to microcosm experiments. Soil slurries at an *in situ* pH of ~4.4 were prepared with 10 g of soil and 3 volumes of deionized water in 125-ml infusion flasks, sealed with gas-tight rubber stoppers and 100% argon in the gas phase. Experiments were done in triplicate. Microcosms were always incubated at 20°C in the dark, which is in the range of temperatures occurring *in situ* (air temperatures of up to 27°C in the month of sampling). Acetylene inhibits the reduction of N_2O to N_2 by blocking nitrous oxide reductases (72). Parallel microcosms with and without acetylene (15% [vol/vol] in headspace) were used to differentiate between total denitrification and N_2O production potentials (72). Experiments without supplemental nitrate or nitrite were conducted to assess denitrification potentials from internal nitrate or nitrite with and without acetylene. For apparent Michaelis-Menten kinetics, soil was preincubated under anoxic conditions to reduce the amount of internal nitrate and nitrite. Plateauing N_2O production indicated that internal nitrate and nitrite were consumed within 24 and 48 h in 0- to 20-cm and below 20-cm palsa peat soils, respectively (see Fig. 2). Preincubated soil was supplemented with 0 to 1,000 μM $NaNO_2$ or $NaNO_3$ or with 0 to 4 μM N_2O. Headspace concentrations of N_2O were determined four or five times via gas chromatography within 8 to 14 h of incubation, and N_2O production and consumption rates were calculated in the linear phase by linear regression of three or four data points (R^2 values were always greater than 0.80). Michaelis-Menten constants (K_m) and the maximum reaction velocities (v_{max}) of denitrification and N_2O consumption were based on the production of N_2O in microcosms supplemented with either nitrate or nitrite and acetylene or on the consumption of N_2O in microcosms supplemented with N_2O. Apparent Michaelis-Menten kinetics were fitted to the data points using the program SigmaPlot, version 10.0 (Systat Software GmbH, Erkrath, Germany) for calculation of K_m and v_{max} according to the following equation (61): $v = (v_{max} \times [S])/(K_m + [S])$ where $[S]$ is the concentration of nitrate or nitrite.

Analytical procedures. Nitrate, nitrite, and ammonium concentrations as well as soil pH and dissolved organic carbon (DOC) were determined in water extracts (10 g of soil in 30 ml of double-distilled H_2O [ddH_2O]; extraction was performed for 24 h at 4°C). Nitrate and nitrite were measured by flow injection analysis using a Dionex DX-500 ion chromatograph equipped with an IonPac AS4A-SC ion exchange column and an ED40 electrochemical detector (Sunnyvale, CA). Ammonium was quantified by flow injection analysis (FIA-LAB; MLE Dresden, Dresden, Germany). Total C and N contents were determined from oven-dried soil with an elemental analyzer (Thermo Quest Flash EA 1112; CE Instruments, Wigan, United Kingdom). DOC was determined after filtration (pore size, 0.45 μm) with a total organic carbon (TOC) analyzer (Multi N/C 2100; Analytik Jena, Jena, Germany). pH was determined with a pH electrode (pH Meter CG 832; Schott Geräte GmbH, Mainz, Germany). Moisture content was obtained by weighing soil samples before and after drying at 60°C for 3 days. N_2O was quantified with a Hewlett-Packard 5980 series II gas chromatograph (Hewlett-Packard, Palo Alto, CA) equipped with an electron capture detector, according to published protocols (48).

Extraction of nucleic acids and PCR amplification of *narG*, *nirK*, *nirS*, and *nosZ*. Nucleic acids were extracted from homogenized soil of each sampled soil layer. Extractions were conducted as described previously with a bead-beating protocol (47). One to two micrograms of DNA was obtained per gram of soil (fresh weight) and had a low humic acid content, as indicated by A_{260}/A_{230} ratios approximating 0.94 to 1.16. *narG*, *nirK*, *nirS*, and *nosZ* were amplified using the primer pairs

narG1960f (TAY GTS GGS CAR GAR AA) and narG2650r (TTY TCR TAC CAB GTB GC) (53), F1aCu (ATC ATG GTS CTG CCG CG) and R3Cu (GCC TCG ATC AGR TTG TGG TT) (68), cd3aF (GTS AAC GTS AAG GAR ACS GG) and R3cd (GAS TTC GGR TGS GTC TTG A) (68), and nosZF (CGC TGT TCI TCG ACA GYC AG) and nosZR (ATG TGC AKI GCR TGG CAG AA) (59), respectively. Each primer was preceded by a 6-base-long bar code (ACACAC for 0- to 20-cm soil; ACGTAC for soil below 20 cm) to separate sequences after pyrosequencing. The application of primers fused to A and B adaptors required for pyrosequencing (which is routinely applied for amplicon pyrosequencing) was avoided to minimize primer bias during PCR (5). PCRs and thermal cycling conditions were as described previously (47).

Bar-coded amplicon pyrosequencing of structural genes. Bar-coded PCR products were gel purified with 1% agarose gels using a Montage Gel Extraction Kit (Millipore Corporation, Bedford, MA), according to the manufacturer's instructions, and purified via isopropanol precipitation to remove residual running buffer. Concentrations of the gel-purified PCR products were determined using Quant-iT PicoGreen (Invitrogen, Carlsbad, CA) and an FLx800 Fluorescence Microplate Reader (BioTek, Bad Friedrichshall, Germany). PCR products (i.e., amplicons) of similar lengths of both soil layers were combined in equal amounts (i.e., *narG* and *nosZ* were pooled, as well as *nirK* and *nirS*). Amplicon mixtures were treated with PreCR Repair Mix (New England BioLabs, Frankfurt am Main, Germany) to eliminate possible PCR-blocking DNA damage that might have occurred during gel purification or storage of amplicons and purified via isopropanol precipitation. A and B sequencing adaptors (GCC TCC CTC GCG CCA TCA G and GCC TTG CCA GCC CGC TCA G, respectively) that are required for pyrosequencing were ligated to the amplicons and sequenced from 5′ (forward) and 3′ (reverse) ends of amplicons. Amplicons were mixed with other samples and subjected to two pyrosequencing analyses at the Göttingen Genomics Laboratory employing a Roche GS-FLX 454 pyrosequencer and GS FLX titanium series reagents (Roche, Mannheim, Germany), according to the manufacturer's instructions. Pyrosequencing runs including *narG* and *nosZ* amplicons yielded 120,775 sequences with a mean sequence length of 372 bp; runs including *nirK* and *nirS* amplicons yielded 173,163 sequences with a mean sequence lengths of 388 bp.

Sequence filtering and analysis. Pyrosequencing and PCR amplification errors can artificially inflate detected sequence diversity (41, 56). Thus, correction or removal of so-called noisy reads is essential to correctly estimate the number of operational taxonomic units (OTUs) in an environmental sample. The AmpliconNoise pipeline achieves reduction of pyrosequencing and PCR amplification errors by flowgram and sequence preclustering, respectively (utilizing the PyroNoise and SeqNoise algorithms, respectively) (56). However, studies have shown that the effect of OTU overestimation becomes less severe at greater clustering distances (33, 41). To assess the effect of pyrosequencing errors on detected diversity of denitrification-related structural gene markers, pyrosequencing reads were clustered (i.e., assigned to OTUs) with and without prior denoising of the data. Undenoised sequences were analyzed using the JAguc2 pipeline (http://wwwagak.informatik.uni-kl.de/research/JAguc/) as described previously (46, 47), while denoising of pyrosequencing reads and subsequent analysis of the denoised sequences were conducted using the AmpliconNoise and Qiime pipelines (10, 56). Sequences with ambiguities and errors in primer or bar code sequences were discarded in both types of analysis. For JAguc2 clustering, *narG* as well as *nosZ* sequences shorter than 350 bp and *nirK* as well as *nirS* sequences shorter than 300 bp were excluded from further analysis. More than 130 bases of forward and reverse reads of nitrite reductase genes (i.e., *nirK* or *nirS*) overlapped. Thus, reverse complements of reverse reads were analyzed together with forward reads. DNA sequences were sorted according to their bar codes and primers, and each subset of sequences was clustered by average linkage clustering after pairwise sequence alignment as this clustering method is rather insensitive to pyrosequencing errors (41). Denoised sequences were aligned using the Needleman-Wunsch algorithm and likewise clustered by an average linkage algorithm. Clustering was redone at different threshold similarities to test the stability of the clusters for the original and the denoised sequence sets.

Denoised data sets were used for subsequent analysis of the denitrification-related structural gene markers. Sequences were assigned to OTUs at species-level threshold distances of 33% (*narG* [49]), 17% (*nirK* [P. Depkat-Jakob et al., unpublished data]), 18% (*nirS* [P. Depkat-Jakob et al., unpublished]), or 20% (*nosZ* [49]) and at 3% sequence difference for each gene marker to allow for comparison of higher-resolved diversity in high-quality data sets. The closest relatives of cluster representatives were determined using BLAST (1). Cluster representatives were edited, translated *in silico*, and aligned with reference sequences using the ClustalW algorithm implemented in MEGA, version 5.0 (40). The alignments were refined manually, and phylogenetic trees were constructed with the neighbor-joining algorithm using *p*-distances from *in silico* translated sequences with MEGA, version 5.0. A total of 10,000 bootstrap replicates were calculated to test the stability of tree topologies (60). OTU tables were rarified; i.e., subsampled OTU tables were created by random sampling at sampling depths of 1,000, 3,000, 80, and 1,000 for *narG*, *nirK*, *nirS*, and *nosZ*, respectively (100 iterations), to remove heterogeneity in sequence numbers obtained from the two soil layers and to estimate the uncertainty in diversity measures. Alpha- and beta-diversity measures and statistical tests were calculated with Qiime from such rarified OTU tables at species-level and at 3% threshold distance (i.e., 97% similarity) for each gene.

Quantification of *narG*, *nirK*, *nirS*, *nosZ*, and 16S rRNA genes in soil. Quantitative kinetic real-time PCRs (qPCRs) were performed as described previously in six technical replicates (47). Gene copy numbers were corrected for inhibition (73). Inhibition factors ranged from 0.5 to 1.0, 0.2 to 0.4, 0.2 to 1.0, 0.8 to 1.0, and 0.5 to 0.6 for qPCR analyses of *narG*, *nirK*, *nirS*, *nosZ*, and 16S rRNA genes, respectively.

Nucleotide sequence accession numbers. The OTU representatives of *narG*, *nirK*, *nirS*, and *nosZ* gene sequences derived from bar-coded amplicon pyrosequencing were deposited at EMBL under accession numbers HE616587 to HE616628. Complete amplicon sequence libraries were deposited in the European Nucleotide Archive (ENA) Sequence Read Archive under study number ERP001096 (http://www.ebi.ac.uk/ena/data/view/ERP001096).

RESULTS

Soil parameters. Soil moisture content of vegetated palsa peat soil was 74% ± 0.3% (Table 1). Soil pH was 4.6 and 4.2 in water extracts from 0- to 20-cm and below-20-cm palsa peat soils, respectively (Table 1). Nitrate and nitrite were below the detection limit (i.e., <0.08 μmol per gram, dry weight [g_{DW}^{-1}], and 0.17 μmol g_{DW}^{-1}, respectively). Ammonium was 125 μM and 106 μM in 0- to 20-cm and below-20-cm palsa peat soils, respectively (Table 1). Dissolved organic carbon was higher in upper than in lower soil layers; total carbon and nitrogen contents were similar in both soil layers, and C/N ratios were 29 and 26 in 0- to 20-cm and below-20-cm soil, respectively (Table 1).

***In situ* gas emissions of vegetated palsa peat soil.** Mean N_2O emissions from unfertilized palsa peat soil were rather small (Fig. 1). However, N_2O fluxes varied from 0.01 to −0.02 μmol of N_2O m^{-2} h^{-1}, indicating that individual palsas can be either sources or sinks for N_2O. Ammonium did not significantly increase N_2O emission from palsa peat soil ($P = 0.6$) (Fig. 1). Initial N_2O emission from nitrate-fertilized palsa peat soil was significantly higher than from unfertilized or ammonium-fertilized palsa peat soil ($P < 0.05$ and $P < 0.01$, respectively), and 1.6 μmol of N_2O m^{-2} accumulated in gas chambers within 3 h following nitrate fertilization (Fig. 1).

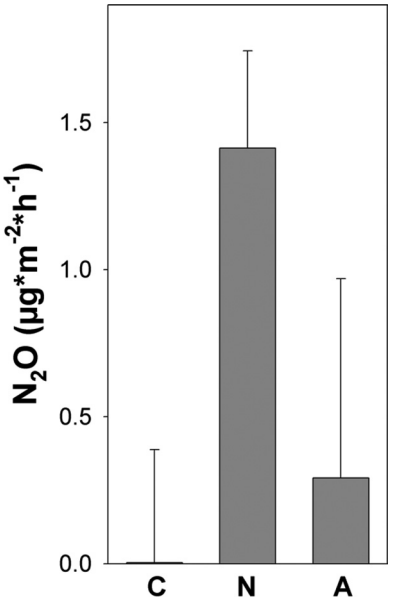

FIG 1 Effect of nitrate and ammonium fertilization on *in situ* fluxes of N_2O from palsa peat soil within 3 h following fertilization (see Materials and Methods for details). Mean values and standard errors of four replicates are shown for unfertilized controls (C) and for treatments fertilized with a solution of 20 mM $NaNO_3$ (N) or 20 mM NH_4Cl (A).

Denitrification activities in palsa peat soil microcosms. N_2O was produced in anoxic microcosms at an *in situ* pH of 4.5 with unsupplemented palsa peat soil from 0 to 20 cm and below 20 cm of depth in the absence of acetylene, and 0.4 and 1 nmol of N_2O g_{DW}^{-1} accumulated during the first 52 h (t_{52}) of incubation, respectively (Fig. 2). N_2O was subsequently consumed in microcosms without acetylene within the next 115 h (t_{167}) of incubation in microcosms with palsa peat soil from below 20 cm, whereas only minor N_2O consumption occurred in microcosms with 0- to 20-cm palsa peat soil ($P = 0.001$ and $P = 0.07$, respectively, for comparison of t_{52} and t_{167}). Below-20-cm palsa peat soil consumed N_2O in atmospheric and subatmospheric concentrations and reduced the concentration from 343 ppb (52 h) to 57 ppb (167 h) (Fig. 2).

Acetylene stimulated the accumulation of N_2O in such microcosms ($P = 0.02$) (Fig. 2); 0.5 and 2 nmol of N_2O g_{DW}^{-1} accumulated in the presence of acetylene within the first 96 h of incubation in microcosms with 0- to 20-cm and below-20-cm palsa peat soils, respectively. N_2O concentrations remained constant after 96 h (t_{96}) of incubation ($P = 0.2$ and $P = 0.3$ for comparison of t_{96} and t_{167}), indicating that all endogenous nitrate or nitrite had been consumed. The amount of N_2O that accumulated in the presence of acetylene indicates that the initial concentration of nitrate/nitrite was at least 0.07 and 0.24 µM (1.1 and 4.0 nmol g_{DW}^{-1}) in 0- to 20-cm and below-20-cm palsa peat soils, respectively. The collective microcosm data suggest that N_2 accounted for approximately 50 to 90% of the gaseous denitrification products at *in situ* pH and nitrate/nitrite concentrations.

Effect of supplemental N oxides on denitrification and N_2O consumption. Nitrate stimulated the production of N_2O in microcosms with palsa peat soil from 0 to 20 cm and below 20 cm of depth ($P \leq 0.03$ for all nitrate concentrations). N_2O production in nitrate-supplemented microcosms was less than 25% of the N_2O production in nitrite-supplemented microcosms (see Fig. S1 in the supplemental material). N_2O production rates in acetylene-amended microcosms with palsa peat soil from both depths increased with increasing nitrate concentrations in the range of 0 to

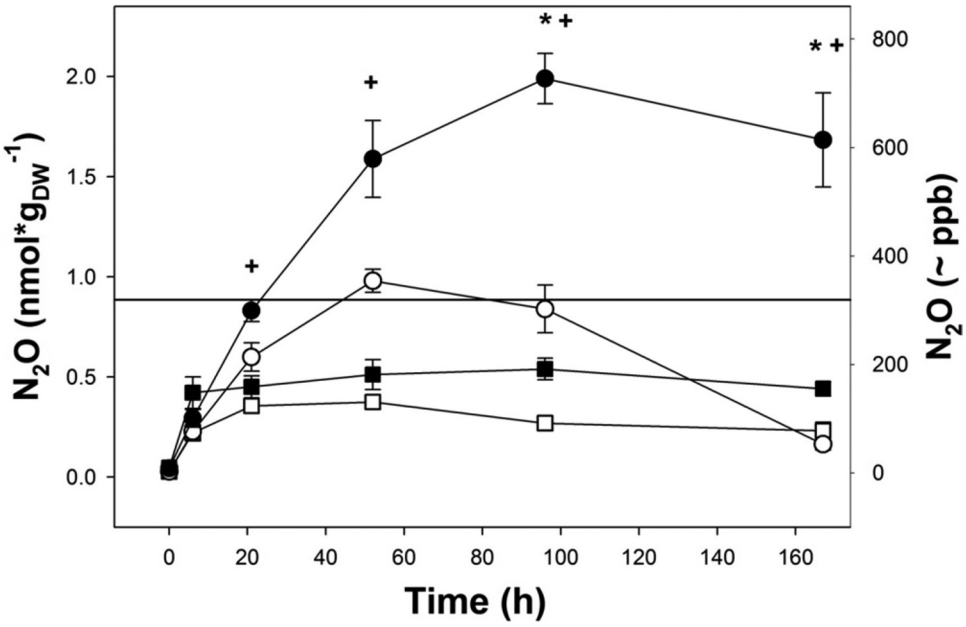

FIG 2 Production and consumption of N_2O by unsupplemented palsa peat soil. Squares and circles represent 0- to 20-cm and below-20-cm palsa peat soils, respectively. Closed and open symbols represent microcosms with and without acetylene, respectively. Mean values and standard errors of three replicates are shown. Time points at which N_2O concentrations in below-20-cm soil with acetylene differed significantly ($P < 0.05$) from N_2O concentrations in below-20-cm soil without acetylene (*) or in 0- to 20-cm palsa peat soil with acetylene (+) are indicated. The horizontal line indicates the atmospheric N_2O concentration (319 ppb).

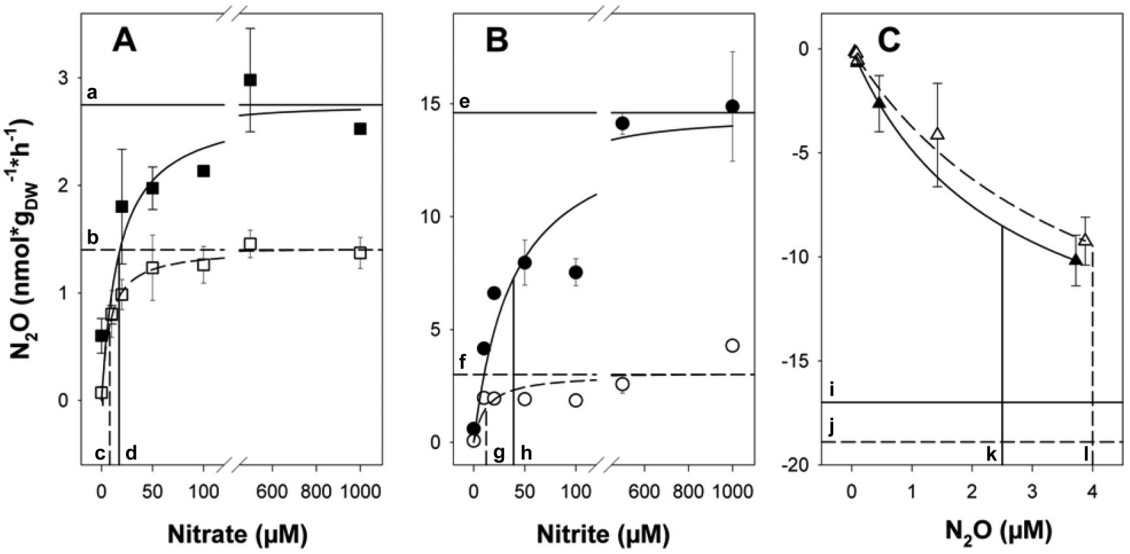

FIG 3 Apparent Michaelis-Menten kinetics of nitrate-dependent (A) and nitrite-dependent (B) N_2O production in the presence of acetylene and N_2O consumption (C) in anoxic palsa peat soil microcosms. Squares, circles, and triangles represent microcosms supplemented with nitrate, nitrite, and N_2O, respectively. Closed and open symbols represent 0- to 20-cm and below-20-cm palsa peat soils, respectively. The *x* axis displays the amount of supplemented (i.e., additional) nitrate, nitrite, or N_2O. Mean values and standard errors of three replicate microcosms are shown. Solid and dashed lines are indicative of 0- to 20-cm and below-20-cm palsa peat soils, respectively. Curves represent Michaelis-Menten fits of the data. Horizontal and vertical lines represent v_{max} and K_m values, respectively. Letters indicate the following values: (i) nitrate-dependent v_{max} (a, 2.75; b, 1.4) and K_m (c, 8.1; d, 17.3), (ii) nitrite-dependent v_{max} (e, 14.6; f, 3.0) and K_m (g, 12.3; h, 39.1), and (iii) N_2O-dependent v_{max} (i, −17.0; j, −18.9) and K_m (k, 2.5; l, 4.0).

50 μM supplemental nitrate and essentially leveled off for nitrate concentrations greater than 50 μM, indicating that denitrifiers in palsa peat are saturated with 50 μM nitrate (Fig. 3A). N_2O production in microcosms with 0- to 20-cm palsa peat soil was about twice as high as in microcosms with below-20-cm palsa peat soil, indicating a greater denitrification potential in the upper soil layer. The ratio of N_2O to combined N_2 and N_2O approximated 50% and 60% for all supplied nitrate concentrations in microcosms with 0- to 20-cm and below-20-cm palsa peat soils, respectively (see Fig. S2), indicating that a substantial portion of N_2O was reduced to N_2 by denitrification.

Supplemental nitrite likewise stimulated the production of N_2O without apparent delay in anoxic microcosms with palsa peat soil ($P \leq 0.02$ for all nitrite concentrations) (see Fig. S1 in the supplemental material). N_2O production rates increased with increasing nitrite concentrations in the range of 0 to 500 and 0 to 20 μM supplemental nitrite for soil from 0 to 20 cm and below 20 cm, respectively (Fig. 3B). N_2O production was higher in 0- to 20-cm soil microcosms than in below-20-cm soil microcosms, underlining the higher denitrification potential of the upper soil layer. The ratio of N_2O to combined N_2 and N_2O varied from 70% to 90% in microcosms with palsa peat soil from both soil layers for all nitrite concentrations (see Fig. S2), indicating that N_2O consumption capacities were in similar ranges when nitrate or nitrite was supplied as an electron acceptor.

Supplemental N_2O was consumed in microcosms with palsa peat soil from both layers (Fig. 3C). Increasing N_2O concentrations stimulated consumption. N_2O consumption rates were similar in microcosms with palsa peat soil from 0 to 20 cm and below 20 cm. Palsa peat soil showed the potential to reduce supplied N_2O to subatmospheric concentrations in such experiments (i.e., approximately 1,000 ppb of N_2O was reduced to 280 ppb within 10 h [data not shown]). Initial N_2O production rates of palsa peat soil microcosms amended with nitrate or nitrite in the presence of acetylene or N_2O consumption rates in the absence of acetylene followed apparent Michaelis-Menten kinetics in both soil layers (Fig. 3). Apparent maximal reaction velocities (v_{max}) were highest for N_2O consumption and higher for nitrite than for nitrate-dependent N_2O production (Fig. 3).

Effect of pyrosequencing and PCR errors on detected diversity of structural gene markers. Denoising of the pyrosequencing reads prior to OTU assignment reduced the number of detected OTUs for all tested gene markers (see Fig. S3 in the supplemental material). The reduction of the OTU number was especially pronounced at small clustering distances (see Fig. S3). At 0% clustering distance, OTU numbers of the original sequence sets were 9 to 30 times higher than OTU numbers of denoised sequence sets. The number of detected OTUs declined rapidly with increasing clustering distance, and similar OTU numbers were obtained for original and denoised sequence sets at clustering distances of 5 to 10% (see Fig. S3).

Phylogenetic analysis of denitrifiers. In total, 28,570 denoised, quality-filtered sequences of the structural gene markers *narG*, *nirK*, *nirS*, and *nosZ* (3,571 ± 751 sequences per gene marker and soil layer on average) were obtained. Forward and reverse reads for *nirK* and *nirS* (amplicon lengths of approximately 470 and 410 bp, respectively) overlapped almost completely and were therefore pooled per gene for further analyses. As overlaps of forward and reverse reads of *narG* and *nosZ* amplicons (amplicon lengths of approximately 670 and 700 bp, respectively) were not sufficient, they were analyzed separately. More than 99% of analyzed sequences generated from amplicons of a certain gene-specific (i.e., *narG*, *nirK*, *nirS*, and *nosZ*) primer set were affiliated with the target gene. Coverage levels of all amplicon libraries were greater than 99% when sequence dissimilarity thresholds of 33%, 17%, 18%, and 20% for *narG*, *nirK*, *nirS*, and *nosZ*, respectively,

TABLE 2 Analysis of *narG*, *nirK*, *nirS*, and *nosZ* derived from palsa peat soil based on two distinct threshold similarities utilized for calling OTUs

Gene marker (read)	Threshold similarity (%)	Soil layer (cm)	No. of sequences	Good's coverage (%)[a]	No. of OTUs observed	No. of OTUs estimated[b]	H^c	E^d
narG (forward)	67	0 to 20	2,956	100.0	4	4 (4–4)	0.56	0.28
		>20	1,925	100.0	3	3 (3–3)	0.81	0.51
	97	0 to 20	2,956	92.1	165	284 (232–375)	3.39	0.46
		>20	1,925	94.7	67	157 (103–293)	2.21	0.36
narG (reverse)	67	0 to 20	3,541	100.0	2	2 (2–2)	0.01	0.01
		>20	1,774	100.0	1	1 (1–1)	0.00	n.a.
	97	0 to 20	3,541	97.0	195	417 (325–576)	3.22	0.42
		>20	1,774	97.9	73	117 (92–172)	2.47	0.40
nirK	83	0 to 20	8,313	100.0	4	4 (4–4)	1.49	0.75
		>20	3,299	99.9	8	9 (8–16)	0.71	0.24
	97	0 to 20	8,313	99.9	34	40 (35–61)	2.33	0.46
		>20	3,299	99.4	48	67(54–105)	1.72	0.31
nirS	82	0 to 20	85	100.0	4	4 (4–4)	0.78	0.25
		>20	833	99.6	12	15 (12–37)	2.39	0.75
	97	0 to 20	85	97.5	7	8 (7–15)	1.09	0.39
		>20	833	97.4	46	85 (59–159)	3.36	0.61
nosZ (forward)	80	0 to 20	1,563	99.9	5	5 (5–5)	1.30	0.56
		>20	1,044	99.9	6	6 (6–6)	1.47	0.58
	97	0 to 20	1,563	99.5	32	38 (33–59)	2.24	0.45
		>20	1,044	99.3	25	29 (26–44)	2.37	0.51
nosZ (reverse)	80	0 to 20	1,856	100.0	4	4 (4–4)	1.27	0.63
		>20	1,381	99.9	6	6 (6–6)	1.45	0.56
	97	0 to 20	1,856	99.6	29	33 (30–51)	2.03	0.42
		>20	1,381	99.5	27	32 (28–55)	2.32	0.49

[a] Percent library coverage (Good's coverage): $C = (1 - n_s/n_t) \times 100$, where n_s is the number of OTUs that occur only once and n_t is the total number of sequences.
[b] Chao1 richness estimate with upper and lower 95% confidence intervals given in parentheses.
[c] Shannon diversity index.
[d] Species evenness.

were utilized for calling OTUs (Table 2). The mean coverage was 98% (ranging from 92 to 100%) when OTUs were called at a 3% sequence dissimilarity threshold, indicating that the number of quality-filtered sequences generated was sufficient for subsequent analyses.

Forward reads of *narG* amplicons yielded more OTUs than reverse reads although similar numbers of sequences were obtained, indicating that the utility of the 3′ ends of *narG* amplicons is higher for diversity analysis than 5′ ends (Table 2; see also Table S1 in the supplemental material). However, results obtained from reverse reads show similar overall trends (Table 2; see also Table S1 and Fig. S4 and S5 in the supplemental material). Thus, information presented below refers to forward reads only. In total, *narG* sequences were assigned to four species-level OTUs (Table 2). Four and three OTUs were detected in palsa peat soil from 0 to 20 cm and below 20 cm, respectively. OTU representatives were only distantly related to publicly available *narG* sequences (sequence dissimilarities ranged from 16 to 33%), indicating phylogenetic novelty. OTU 1 affiliated with actinobacterial *narG*, while OTU 2 affiliated with alphaproteobacterial *narG* (Table 3; see also Fig. S4). OTUs of *narG* from palsa peat soil were related to *narG* genes of uncultured bacteria from upland and fen soil as well as from sediments and to *narG* genes of *Methylocella sylvestris*, *Actinosynnema mirum*, *Rubrobacter xylanophilus*, *Oligotropha carboxidovorans*, and *Desulfurispirillum indicum* (Table 3; see also Fig. S4). OTU 1 dominated *narG* in both layers and accounted for 87% and 76% of the sequences in 0- to 20-cm and below-20-cm soil, respectively, while OTU 2 accounted for 13% and 24% of the sequences in 0- to 20-cm and below-20-cm soil, respectively (Table 3; see also Fig. S4). Rarefaction analysis (i.e., random subsampling of each amplicon library) was applied to minimize the potential bias introduced by varying the numbers of sequences per amplicon library. OTUs called at species-level threshold distances of 33% were split into several OTUs at a 3% threshold distance in original and rarified data sets (Fig. 4 and Table 2; see also Table S1 in the supplemental material). In rarified data sets, *narG* sequences were likewise assigned to four OTUs at a 33% species-level threshold distance, which were split into 111 3%-OTUs (at a 3% threshold distance); 85, 22, 2, and 1 3%-OTUs were derived from sequences of 33%-OTUs 1, 2, 3, and 4, respectively. *narG* community composition differed between soil layers at a 3% threshold distance; 3%-OTU 1.1 dominated *narG* in 0- to 20-cm palsa peat soil, while 3%-OTU 1.2 dominated *narG* in below-20-cm palsa peat soil (Fig. 4). Differences in observed and estimated OTU numbers were rather insignificant at the 33% species-level threshold distance when rarified data sets were utilized (see Table S1). Shannon diversity indices, species evenness, and Chao1 richness estimates of *narG* from 0- to 20-cm and below-20-cm palsa peat soils were significantly different at a 3% threshold difference; alpha-diversity of *narG* tended to be higher in soil

TABLE 3 Amino acid identities of *in silico* translated OTU representatives of denitrification-associated genes retrieved from acidic palsa peat soil to closely related sequences

Gene (read)[b]	OTU no. (accession no.)	Closest relative		Closest cultured relative		Relative abundance of OTUs in amplicon libraries (%)	
		Name (accession no.)	Identity (%)[a]	Name (accession no.)	Identity (%)[a]	0 to 20 cm	Below 20 cm
narG (forward)	1 (HE616587)	Uncultured bacterium (AY955190)	82	*Streptomyces coelicolor* A3(2) (NC 003888)	78	87.3	75.8
	2 (HE616588)	*Oligotropha carboxidovorans* OM 5 (CP001196)	84	*Oligotropha carboxidovorans* OM 5 (CP001196)	84	12.6	24.1
	3 (HE616589)	Uncultured bacterium (FJ556609)	68	*Oceanithermus profundus* DSM 14977 (CP002361)	64	0.03	0.1
	4 (HE616590)	*Rubrobacter xylanophilus* DSM 9941 (CP000386)	72	*Rubrobacter xylanophilus* DSM 9941 (CP000386)	72	0.07	0
narG (reverse)	1 (HE616591)	Uncultured bacterium (AY955190)	86	*Actinosynnema mirum* DSM 43827 (CP001630)	75	99.9	100
	2 (HE616592)	*Nitrobacter hamburgensis* X14 (NC 007964)	71	*Nitrobacter hamburgensis* X14 (NC 007964)	71	0.1	0
nirK[c]	1 (HE616593)	Uncultured bacterium (DQ783977)	97	*Bradyrhizobium* sp. strain ORS278 (NC 009445)	84	57.6	0.33
	2 (HE616594)	Uncultured bacterium (EF623499)	78	*Rhodopseudomonas palustris* BisA53 (CP000463)	76	12.8	82.9
	3 (HE616595)	Uncultured bacterium (DQ304355)	96	*Bradyrhizobium* sp. strain GSM-467 (FN600568)	85	26.6	0.09
	4 (HE616596)	Uncultured bacterium (EU790857)	80	*Alcaligenes* sp. strain I (DQ108983)	79	0	16.4
	5 (HE616597)	Uncultured bacterium (EU790858)	92	*Bosea* sp. MF18 (EF363545)	92	2.9	0
	6 (HE616598)	Uncultured bacterium (DQ783907)	82	*Bradyrhizobium* sp. strain D203a (AB480454)	76	0	0.12
	7 (HE616599)	Uncultured bacterium (DQ783888)	85	*Bradyrhizobium* sp. strain BTAi1 (NC 009485)	81	0	0.06
	8 (HE616600)	Uncultured bacterium (EF623499)	77	*Methylobacterium* sp. strain R-25207 (AM230850)	75	0	0.03
	9 (HE616601)	Uncultured bacterium (EU790858)	79	*Rhizobium etli* CFN 42 (NC 007766)	78	0	0.03
nirS[d]	1 (HE616602)	Uncultured bacterium (GQ443982)	92	*Rubrivivax gelatinosus* (AB536930)	80	0	36.2
	2 (HE616603)	Uncultured bacterium (GU393200)	86	*Pseudomonas* sp. strain I-Bh25-14 (FN555560)	75	0	31.6
	3 (HE616604)	Uncultured bacterium (GU393229)	87	*Bradyrhizobium* sp. strain TSA26 (AB542313)	84	86.3	8.5
	4 (HE616605)	Uncultured bacterium (GU393213)	88	*Thiobacillus denitrificans* ATCC 25259 (CP000116)	76	0	9.0
	5 (HE616606)	Uncultured bacterium (HM438800)	95	*Dechlorospirillum* sp. strain I-Bh37-22 (FN555562)	80	0	5.3
	6 (HE616607)	Uncultured bacterium (DQ676123)	85	*Thiobacillus denitrificans* ATCC 25259 (CP000116)	80	0	4.6
	7 (HE616608)	Uncultured bacterium (DQ676123)	84	*Aromatoleum aromaticum* EbN1 (NC 006513)	78	0	3.1
	8 (HE616609)	Uncultured bacterium (GU393183)	78	*Cupriavidus* sp. strain TSA25 (AB542312)	74	0	0.84
	9 (HE616610)	Uncultured bacterium (GU393076)	92	*Bradyrhizobium* sp. strain TSA1 (AB542304)	86	6.3	0
	10 (HE616611)	Uncultured bacterium (GU393229)	87	*Rhodanobacter* sp. strain D206a (AB480490)	85	5.0	0.12
	11 (HE616612)	Uncultured bacterium (AY583422)	89	*Cupriavidus metallidurans* CH34 (CP000352)	77	0	0.48
	12 (HE616613)	Uncultured bacterium (GU393076)	94	*Bradyrhizobium* sp. strain TSA1 (AB542304)	87	2.5	0
	13 (HE616614)	Uncultured bacterium (DQ303103)	84	*Rhodanobacter* sp. strain D206a (AB480490)	82	0	0.12
	14 (HE616615)	Uncultured bacterium (DQ676123)	82	*Cupriavidus* sp. strain N24 (AB480486)	78	0	0.12
nosZ (forward)	1 (HE616616)	Uncultured bacterium (FN430557)	96	*Oligotropha carboxidovorans* OM 5 (CP001196)	85	51.1	51.9
	2 (HE616617)	Uncultured bacterium (FN430533)	91	*Burkholderia pseudomallei* K96243 (BX571965)	90	43.4	37.6
	3 (HE616618)	Uncultured bacterium (FN430550)	87	*Pseudomonas brassicacearum* PD 5 (DQ377777)	82	3.8	8.1
	4 (HE616619)	*Alcaligenes faecalis* A15 (AF361795)	95	*Alcaligenes faecalis* A15 (AF361795)	95	1.5	1.0
	5 (HE616620)	*Azospirillum* sp. TSO41-3 (AB545691)	83	*Azospirillum* sp. strain TSO41-3 (AB545691)	83	0	1.2
	6 (HE616621)	Uncultured bacterium (FN430537)	90	*Azospirillum brasilense* SpT60 DSM 2298 (AF361792)	90	0.06	0
	7 (HE616622)	Uncultured bacterium (FN430542)	89	*Burkholderia pseudomallei* K96243 (BX571965)	87	0	0.1
nosZ (reverse)	1 (HE616623)	Uncultured bacterium (FN430557)	95	*Rhodopseudomonas palustris* HaA2 (CP000250)	81	52.3	52.1
	2 (HE616624)	Uncultured bacterium (FN430533)	91	*Azospirillum lipoferum* (AF361793)	85	42.4	36.5
	3 (HE616625)	Uncultured bacterium (FN430533)	87	*Mesorhizobium* sp. strain TSA41b (AB542285)	79	4.7	10.0
	4 (HE616626)	*Ralstonia solanacearum* GMI1000 (AL646053)	85	*Ralstonia solanacearum* GMI1000 (AL646053)	85	0.59	0.36
	5 (HE616627)	Uncultured bacterium (FJ209438)	83	*Mesorhizobium* sp. strain D246 (AB480521)	76	0	0.94
	6 (HE616628)	*Bradyrhizobium japonicum* USDA 110 (BA000040)	88	*Bradyrhizobium japonicum* USDA 110 (BA000040)	88	0	0.07

[a] Determined after alignment in MEGA, version 5.0.
[b] Where indicated, analyses were based on forward or reverse reads.
[c] Analyses included forward and reverse complements of reverse reads; minimal sequence overlaps of forward and reverse reads were 130 bases.
[d] Analyses included forward and reverse complements of reverse reads; minimal sequence overlaps of forward and reverse reads were 190 bases.

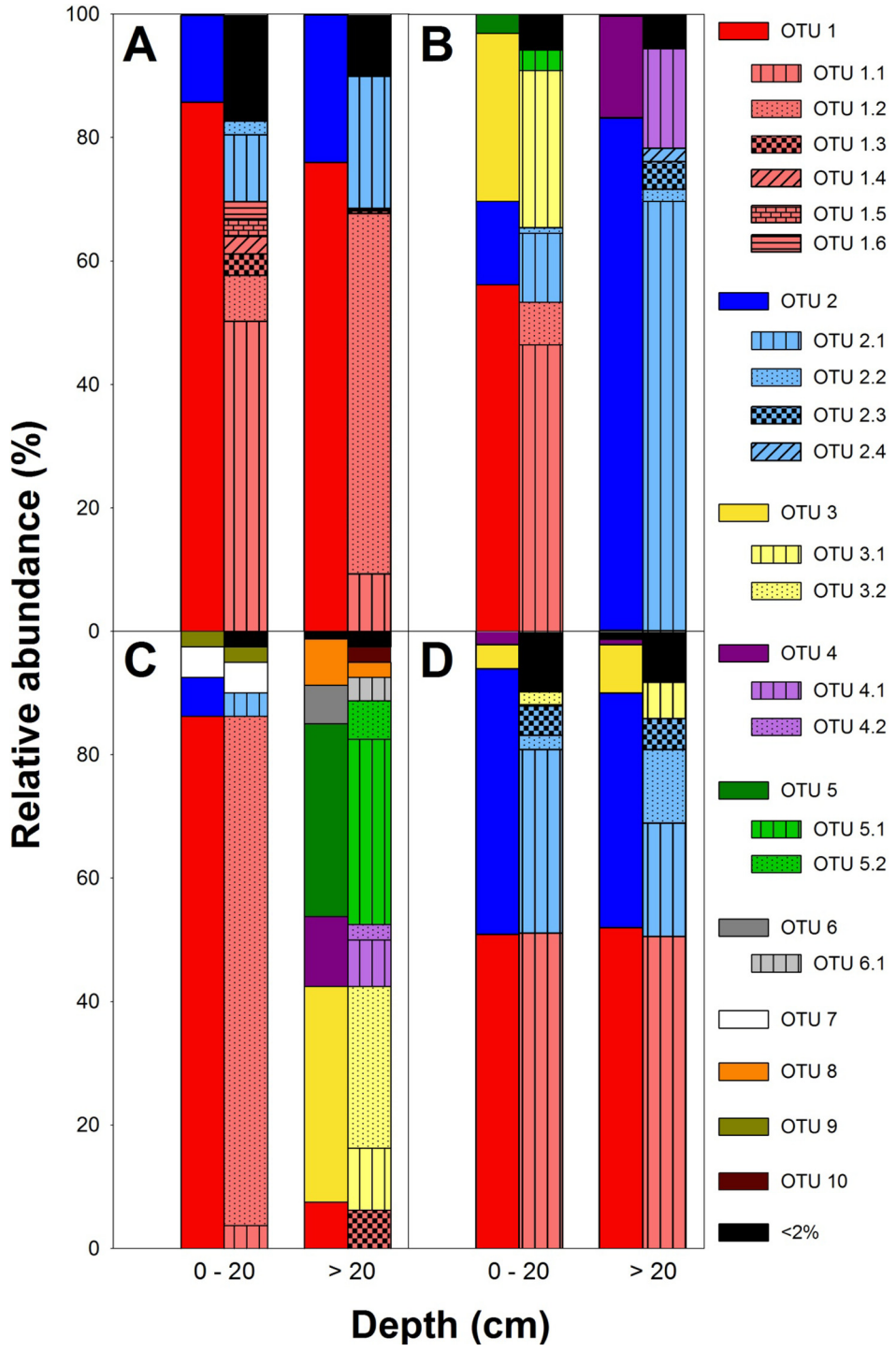

FIG 4 Relative abundances of OTUs derived from *narG* forward reads (A), *nirK* (B), *nirS* (C), and *nosZ* forward reads (D) retrieved from palsa peat soil at species level (left bars) and at 3% (right bars) threshold distances from rarified data sets. OTUs were rarified at sampling depths of 1,000, 3,000, 80, and 1,000 for *narG*, *nirK*, *nirS*, and *nosZ*, respectively. OTUs called at species-level threshold distances were enumerated 1 through 10; subclusters of those OTUs called at 3% threshold distance were enumerated 1.1 through 6.1. All OTUs that had relative abundances below 2% in both layers were grouped. Please note that the same color coding for different structural genes does not indicate whether such genes were derived from the same organisms.

from 0- to 20-cm soil than in soil from below 20 cm (see Table S1). Beta-diversity measures showed larger differences in community composition at 3% than at the 33% threshold distance (see Table S1).

nirK genes were assigned to nine species-level OTUs. Four and eight OTUs were detected in palsa peat soils from 0 to 20 cm and from below 20 cm, respectively (Table 2). OTUs 1 and 2 dominated *nirK* in palsa peat soils from 0 to 20 cm and below 20 cm,

respectively (about 58% and 83%, respectively). OTU 3 accounted for 27% of *nirK* in palsa peat soil from 0 to 20 cm but for only 0.1% of *nirK* from below-20-cm palsa peat soil, while OTU 4 accounted for 16% of *nirK* from below-20-cm palsa peat soil but was not detected in 0- to 20-cm palsa peat soil (see Fig. S6 in the supplemental material). Sequence dissimilarities of OTU representatives to publicly available *nirK* sequences ranged from 3 to 25%, indicating the presence of new and known denitrifiers in palsa peat soil (Table 3). All *nirK* detected in palsa peat soil affiliated with alphaproteobacterial *nirK*. OTUs 2, 4, and 8 were related to *nirK* of uncultured bacteria and more distantly related to *nirK* of *Methylobacterium* sp., while OTUs 1 and 3 were related to *nirK* of *Bradyrhizobium* sp. and *Rhodopseudomonas* sp. (Table 3; see also Fig. S6). In rarified data sets, *nirK* sequences were likewise assigned to 9 OTUs at a 17% species-level threshold distance which were split into 67 3%-OTUs; 20, 30, 2, 4, and 3 OTUs were derived from sequences of 17%-OTUs 1, 2, 3, 4, and 5, respectively. Alpha-diversity measures (i.e., Shannon diversity index, species evenness, and Chao1) differed significantly between the two soil layers and suggested a higher diversity of *nirK* in soil from 0 to 20 cm than from soil below 20 cm when rarified data sets were utilized (see Table S1). Beta-diversity measures indicated little overlap of the two communities, confirming the observed OTU patterns (Fig. 4; see also Table S1,).

Fourteen species-level OTUs of *nirS* were detected in the original data set (Table 2). Four and 12 OTUs were detected in 0- to 20-cm and below-20-cm palsa peat soils, respectively (Table 2). *nirS* of palsa peat soil from 0 to 20 cm was dominated by OTUs affiliated with alphaproteobacterial *nirS*, while *nirS* genes from soil below 20 cm were dominated by *nirS* affiliated with betaproteobacterial *nirS* (Table 3; see also Fig. S7 in the supplemental material). Many OTUs were related to *nirS* of uncultured wetland or marine sediment bacteria and distantly related to *nirS* of *Bradyrhizobium* sp. (0 to 20 cm) and other *Alphaproteobacteria* and to *Azoarcus tolulyticus* (below 20 cm) (Table 3; see also Fig. S7). Sequence dissimilarities of OTU representatives to publicly available *nirS* sequences ranged from 5 to 22%, indicating the presence of phylogenetically new denitrifiers in palsa peat soil. In rarified data sets, *nirS* sequences were assigned to 10 OTUs (rather than 14 OTUs for the original data set) at an 18% species-level threshold distance (see Table S1) since the low number of sequences obtained for 0- to 20-cm peat soil limits the number of sequences analyzed from soil below 20 cm of depth. Such 18%-OTUs were split into 19 3%-OTUs; 4, 3, 2, 2, 2, and 2 OTUs were derived from sequences of 18%-OTUs 1, 2, 3, 4, 5, and 6, respectively. The *nirS* community composition differed between soil layers at 18% and 3% threshold distances, and *nirS* genes from OTU 1 were assigned to different 3%-OTUs in the upper and lower soil layers (Fig. 4). Alpha-diversity measures were significantly higher in below-20-cm soil than in 0- to 20-cm soil at both threshold distances; beta-diversity measures indicated little overlap of the two communities when rarified data sets were utilized, as was observed for *nirK* (Fig. 4; see also Table S1).

nosZ forward reads were assigned to seven species-level OTUs. Five and six OTUs were detected in palsa peat soil from 0 to 20 cm and from below 20 cm, respectively (Table 2). OTUs 1 and 2 dominated *nosZ* amplicon libraries of palsa peat soil from both soil layers (see Fig. S8 in the supplemental material). Sequence dissimilarities of OTU representatives to publicly available *nirS* sequences ranged from 4 to 18%, indicating the presence of phylogenetically new denitrifiers capable of N_2O consumption. Essentially all *nosZ* genes were affiliated with alpha- and betaproteobacterial *nosZ* and clustered with *nosZ* of wetland and upland soils, as well as *Bradyrhizobium japonicum* and *Azospirillum lipoferum* (Table 3; see also Fig. S8). *nosZ* reverse reads yielded similar results (Table 2; see also Fig. S9 in the supplemental material). In rarified data sets, *nosZ* sequences formed 6 OTUs at a 20% species-level threshold distance which were split into 39 3%-OTUs; 24, 7, and 5 3%-OTUs were derived from OTUs 1, 2, and 3, respectively. *nosZ* community composition was similar in both soil layers at 20% and 3% threshold distances. However, minor differences in the 3%-OTU composition of 20%-OTUs 2 and 3 were detected (Fig. 4). Alpha-diversity was in general marginally higher in below-20-cm palsa peat soil; beta-diversity measures indicated a higher proportion of shared OTUs and a more common phylogeny than observed for the other gene markers when rarified data sets were utilized (see Table S1).

TABLE 4 Copy numbers of denitrification-associated genes in palsa peat soil

Gene	Copy no. by soil layer			
	From 0–20 cm		Below 20 cm	
	Per 16S rRNA gene (%)[a,g]	Per ng of DNA	Per 16S rRNA gene (%)[b,g]	Per ng of DNA
narG[c]	$(8.9 \pm 0.5) \times 10^{-1}$	$(1.5 \pm 0.1) \times 10^{4}$	$(4.9 \pm 0.4) \times 10^{0}$	$(5.1 \pm 0.2) \times 10^{4}$
nirK[d]	$(1.2 \pm 0.3) \times 10^{-3}$	$(1.4 \pm 0.3) \times 10^{0}$	$(3.3 \pm 0.9) \times 10^{-4}$	$(8.6 \pm 2.3) \times 10^{-1}$
nirS[e]	$(1.6 \pm 0.2) \times 10^{-1}$	$(2.5 \pm 0.3) \times 10^{2}$	$(1.4 \pm 0.3) \times 10^{-2}$	$(3.7 \pm 0.7) \times 10^{1}$
nosZ[f]	$(2.7 \pm 0.5) \times 10^{-3}$	$(4.3 \pm 0.8) \times 10^{1}$	$(8.4 \pm 1.0) \times 10^{-3}$	$(8.8 \pm 0.8) \times 10^{1}$

[a] 16S rRNA gene copy numbers were $(1.6 \pm 0.1) \times 10^{6}$ per ng DNA.
[b] 16S rRNA gene copy numbers were $(1.0 \pm 0.1) \times 10^{6}$ per ng DNA.
[c] Assay validation for *narG:* detection limit, 10^{1} copies; PCR efficiency, 108.2%; standard curve r^2, 0.993.
[d] Assay validation for *nirK:* detection limit, 10^{0} copies; PCR efficiency, 106.0%; standard curve r^2, 0.993.
[e] Assay validation for *nirS:* detection limit, 10^{1} copies; PCR efficiency, 97.5%; standard curve r^2, 0.993.
[f] Assay validation for *nosZ:* detection limit, 10^{1} copies; PCR efficiency, 101.5%; standard curve r^2, 0.989.
[g] Assay validation for 16S rRNA: detection limit, 10^{1} copies; PCR efficiency, 95.9%; standard curve r^2, 0.994.

Quantification of *narG*, *nirK*, *nirS*, and nosZ relative to 16S rRNA genes. Copy numbers of all genes investigated in this study were corrected by inhibition factors that were experimentally determined for every DNA extract and gene analyzed (see Materials and Methods). Copy numbers of *narG* accounted for 1 and 5% of bacterial 16S rRNA gene copy numbers in 0- to 20-cm and below-20-cm palsa peat soils, respectively (Table 4). Copy numbers of *narG*, *nirK*, *nirS*, and *nosZ* were essentially in the same order of magnitude in both soil layers although gene ratios of copy numbers from 0- to 20-cm soil to below-20-cm soil were 0.3, 1.6, 6.8, and 0.5 for *narG*, *nirK*, *nirS*, and *nosZ*, respectively (Table 4), suggesting a tendency for nitrite reductase genes to be more abundant in upper than lower soil layers. *nirS* copy numbers were approximately 100 times higher than *nirK* copy numbers (Table 4). *nosZ* copy numbers were in the same magnitude as *nirS* copy numbers in below-20-cm palsa peat soil while the *nirS* copy numbers were about 10 times higher than *nosZ* copy numbers in 0- to 20-cm palsa peat soil (Table 4).

DISCUSSION

Denitrifiers in palsa peat soil as a source and sink for N_2O. N_2O emission was stimulated *in situ* with nitrate rather than ammo-

nium, and new as well as diverse denitrification-associated genes were abundant, highlighting the importance of denitrifiers for N_2O fluxes in acidic palsa peats (Fig. 1 and Table 2; see also Table S1 and Fig. S4 to S9 in the supplemental material). Although the N_2O flux measurements were performed only once, N_2O emission rates were in the range of those observed for previously analyzed vegetated palsas that were characterized by similar C/N ratios (Table 1) (45). However, unvegetated palsas with C/N ratios similar to those of the vegetated palsa peat emit large amounts of N_2O; such emissions are in the same range as determined for agricultural and tropical soils (45, 58, 71). Thus, although the C/N ratio is recognized as a strong determinant for N_2O emission, it is not the sole determinant for N_2O emission capabilities of peatlands (38). Unvegetated palsas are characterized by a low ratio of ammonium to nitrate, indicating a good nitrification-derived nitrate supply to denitrifiers (45). In contrast, high ratios of ammonium to nitrate in vegetated tundra peatlands as observed also in Skalluvaara palsa peat (Table 1) indicate restricted nitrification activity and thus low nitrate availability (45). Copy numbers of *narG* and of *nirK* and *nirS* were at the lower end or in the same range of those detected in soil or other permafrost-affected acidic peatlands, respectively (9, 14, and 47), demonstrating that nitrate reducers and denitrifiers were abundant. Nitrate and nitrite stimulated denitrification in palsa peat soil without apparent delay at ratios of 60 to 90% of N_2O to total N gas highlighting N-oxide limitation of denitrifiers (Fig. 3; see Fig. S1 and S2 in the supplemental material), indicating that denitrifiers in palsa might become a significant source of N_2O when nitrate is available. Such data (i) suggest that denitrification rather than nitrification is the major source of N_2O in Skalluvaara palsa peat soil, (ii) indicate that denitrifiers are prone to react to nitrate supply, and (iii) are in line with the hypothesis that N_2O emissions from vegetated permafrost-affected peatlands are low due to nitrification-limited nitrate supply to denitrifiers (45).

Many nitrate-limited denitrifiers hosting N_2O reductases utilize N_2O as a terminal electron acceptor under anoxic conditions (34, 76, 78). Acidic wetlands including vegetated palsa peats represent temporary sinks of atmospheric N_2O, and N_2O consumption of atmospheric levels was detected *in situ* at the Skalluvaara palsa peat site and in microcosms (Fig. 1 and 2) (11, 24, 39, 45, 48). The acetylene inhibition technique indicated that N_2 was a denitrification end product in unsupplemented palsa peat soil microcosms (Fig. 2). Nitrous oxide reductase gene copy numbers were present and low compared to levels in less acidic soils and in the same range as those of acidic tundra soil (9, 14, and 47). The ratio of detected nitrite reductase to N_2O reductase genes approximated 10 and 1 in upper and lower soil layers, respectively (Table 4), suggesting that detected denitrifiers capable of N_2O production outnumbered those capable of N_2O consumption in the upper layer of palsa peat. The ratio of nitrite reductase genes to N_2O reductase genes is highly variable in soils, and often nitrite reductase copy numbers largely exceed N_2O reductase copy numbers (14, 28, 47). Such findings are in agreement with the fact that only approximately two-thirds of the genomes of cultured denitrifiers harbor *nosZ* (35). However, *nosZ* copy numbers in the lower soil layer were similar to those of the upper soil layer, indicating similar genetic potentials to consume N_2O. Such genetic potentials were essentially reflected by the maximal reaction velocities, likewise suggesting (i) higher N_2O production in upper than lower soil layers and (ii) similar N_2O consumption capacities in upper and lower soil layers (Fig. 3). Interestingly, maximal reaction velocities for N_2O consumption exceeded those for N_2O production, and ratios of maximal reaction velocities for N_2O production to N_2O consumption ranged from 0.1 to 0.9 (Fig. 3). Ratios in the same range were observed for acidic to pH-neutral soils in Finland, Sweden, and Germany and demonstrate a high relative capacity of the acidic Skalluvaara peat soil to consume N_2O (30). Given equilibrium concentrations of dissolved N_2O in the range of 10 nM N_2O when 380 ppb of N_2O in the atmosphere is assumed and dissolved N_2O concentrations of up to 8 nM in pore water of a German fen (23), the data indicate that N_2O will be used as a terminal electron acceptor by acid-tolerant palsa peat denitrifiers, especially when the electron acceptors nitrate and nitrite are depleted, allowing palsa peats to act as temporary N_2O sinks.

New denitrifier communities in palsa peat soil differ with depth. Denitrifier diversity was analyzed by bar-coded amplicon pyrosequencing of multiple denitrification-associated structural genes (Table 2; see also Table S1 in the supplemental material). Variability among technical replicate bar-coded amplicon pyrosequencing analyses of 16S rRNA genes might be rather high when OTUs are called at a 97% sequence similarity threshold, and only 30 to 65% of estimated total OTUs are detected, suggesting that bar-coded amplicon pyrosequencing underestimates shared taxa when coverage is low (74). Such variabilities are attributed to primer biases originating from the utilization of primers with different bar codes and might be minimized by applying two-step PCR approaches (5). However, average coverage levels of 99% as obtained for denitrification-associated structural genes (Table 2), utilization of two sequence distances for calling OTUs as well as forward and reverse reads, and rarifying data sets for determining beta-diversity (see Table S1) suggest that artifacts in the denitrification-associated gene-based estimates of denitrifier beta-diversity were minimal. Within the limitations of target gene detectability by the utilized primer sets, tagged amplicon pyrosequencing-based approaches are well suited for capturing the alpha-diversity of detectable microbial communities when rigorous sequence correction algorithms are applied (see Materials and Methods) even if coverage levels are well below 99% (74).

Most detected *narG* sequences from Skalluvaara palsa peat clustered within the *Actinobacteria* and were related to *narG* of *Actinosynnema* sp. (Table 3; see also Fig. S4 in the supplemental material). *Actinosynnema* sp.-related actinobacterial *narG* genes were the dominant group in unturbated peat plateau tundra and cryoturbated peat circles of Russian permafrost-affected peat soil, indicating that this group is common in the nitrate-reducer community of permafrost-affected peatland soils (47). Actinobacterial *narG* genes are predominant in Canadian permafrost soil, and *Actinobacteria* is the dominant taxon in the active layer in Canadian arctic permafrost soil, thus highlighting the importance of *Actinobacteria* in the nitrate reducer community of palsa peats and other permafrost systems (47, 65).

Proteobacteria are abundant in permafrost soils, which is in line with the affiliation of detected *nirK*, *nirS*, and *nosZ* from palsa peat with *Proteobacteria* (see Fig. S6 to 8 in the supplemental material) (65). Since the phylogenies of *nirS* and *nosZ* are basically congruent with 16S rRNA-based phylogenies (29, 35, 49), *Proteobacteria* are suggested as important denitrifiers in permafrost environments. Pronounced differences were detected in the diversity of the nitrite reductase genes between soil layers for *nirK* and *nirS*. Indeed, nitrite reductase communities reflect differences in environmental conditions more strongly than nitrate or N_2O reduc-

tase communities (6, 9, 14, 47). Copy numbers of *nirS* genes (i.e., the predominant detected nitrite reductase genes) were significantly higher in the upper soil layer than in the lower soil layer (Table 4). Such a trend was reflected in the nitrite-dependent kinetic parameters, likewise suggesting dissimilar denitrifier communities in upper and lower soils (Fig. 3). Such findings are supported by recent studies demonstrating a positive correlation of *nirS* and 16S rRNA genes with denitrification potentials (14, 51). Although current PCR-based analyses of nitrate reducer communities including denitrifiers underestimate the real diversity in the environment due to the selectivity of the primers utilized, the collective data represent a minimal estimate of denitrifier diversity and abundance and indicate abundant, diverse, acid-tolerant, and uncultured nitrate reducers including denitrifiers in palsa peat soil (25, 29, 36). The composition of *nirK* and *nirS* OTUs of Skalluvaara palsa peat soil was similar to the community composition in unturbated permafrost-affected tundra peat soil, while especially *nirS* community composition of cryoturbated peat circle soil differed strongly from both unturbated tundra and palsa peat soil (47), indicating site-specific differences in permafrost-nitrite reducer communities that might relate to observed differences in N_2O emissions.

The community composition of detected N_2O-consuming denitrifiers, as indicated by *nosZ* sequence analysis, clearly differed between Finnish palsa peat and Russian tundra peat soil, as *nosZ* genes from Finnish palsa peat soil were dominated by sequences related to *Bradyrhizobium* and *Azospirillum*, while *nosZ* genes from Russian tundra peat soil are dominated by *Mesorhizobium*-related *nosZ* genes (47). N_2O emissions from Russian cryoturbated peat circles are much higher than from palsa peat soil, and ratios of N_2O to N_2 are likewise higher in Russian peat soil (47), indicating that *Mesorhizobium*-related denitrifiers in Russian peat soil, which are absent in Skalluvaara peat soil, might be candidates for key denitrifiers impacting the N_2O consumption capability of permafrost-affected soils.

Predominance of detected *nirS*-type rather than *nirK*-type denitrifiers. Detected genes indicative of cytochrome cd_1-dependent nitrite reductases (i.e., *nirS*) outnumbered genes indicative of copper-dependent nitrite reductases (i.e., *nirK*) by approximately 2 orders of magnitude (Table 4), suggesting that *nirS*-type denitrifiers are important for denitrification in palsa peat. Substantially higher copy numbers of *nirS* than *nirK* are detected in certain (semi-)aquatic habitats and acidic soils by a range of different primers, suggesting that *nirS*-type denitrifiers are well adapted to low pH and high water content (3, 22, 32, 47). However, the primer systems for *nirK* and *nirS* used in this study and many others target mainly diverse *Proteobacteria* excluding recently described *nirK*-hosting acid-tolerant *Rhodanobacter* species (25, 26, 68). Thus, conclusions are limited to detectable proteobacterial *nirK*-type and *nirS*-type denitrifiers. Niche differentiation rather than competitive exclusion is hypothesized as a mechanism for the occurrence of *nirS*-type and *nirK*-type denitrifiers detected with currently available primers (9, 18, 37). Abundance of such *nirS*-type denitrifiers is impacted by pH, nitrate, soil moisture, and manganese content, and a positive correlation of *nirS* abundance and soil moisture was revealed (9, 14, 15, 18, 27), suggesting that moisture content and the low pH might favor putative proteobacterial *nirS*-type denitrifiers in palsa peat soils.

Denitrifier community composition and regulation of N_2O fluxes. The community composition of soil denitrifiers impacts on denitrification capacities, on the response of denitrification to soil pH, and thus on the release of N_2O into the atmosphere (7, 16, 30). Acidic pH impairs the activity of N_2O reductase, most likely by posttranscriptional effects (4, 43). Cells of the neutrophilic model denitrifier *Paracoccus denitrificans* grown under pH-neutral conditions that were subjected to N_2O reduction assays display only 50% of N_2O reduction rates at pH 6.1 compared to a pH of 7.5. Transcription of *nosZ* in cells grown at pH 6.1 is essentially not affected compared to those at pH 7.5, while N_2O reduction capabilities are severely impaired by the low pH (4). Soil denitrifiers likewise show lower N_2O reduction activities at pH 6.1 than at pH 8.0 but higher transcriptional activities of *nosZ* at the lower pH, which might be viewed as an attempt to partially compensate for N_2O reduction activities (43). Thus, current knowledge suggests that the posttranscriptional effects at low pH impairing N_2O reduction activities include negative effects on (i) the activity of the mature N_2O reductase enzyme and (ii) the export/and or assembly of premature N_2O reductases (76).

Indeed, the relative proportion of N_2O in total N gases is higher in acidic than in pH-neutral soil (64). However, denitrifiers adapted to a low pH of their environment occur in certain habitats (16, 48, 50). Some acid-tolerant strains of *Rhodanobacter* sp. (e.g., *Rhodanobacter denitrificans* and *Rhodanobacter thiooxydans*) are capable of complete denitrification to N_2 at pH 4 (i.e., N_2O reduction) and are associated with denitrification in acidic subsurface environments (25, 26, 55, 70). Such findings, half-lives of mature model N_2O reductases during N_2O turnover of approximately 5 min (as reviewed in reference 76), and high N_2O reduction capabilities in palsa peat soil microcosms at pH 4 for greater than 8 h under anoxic conditions (Fig. 3C) argue in favor of a robust acid-tolerant N_2O reducing capability of palsa peat organisms rather than measuring the activity of N_2O reductases that had been expressed in pH-neutral microsites.

Soil pH exerts strong effects on the community composition of soil bacteria, and phylotypic diversity is lower in acidic than in pH-neutral soils (19, 42). Such pH effects are in line with putative new denitrifiers that were detected in palsa peats and other acidic wetlands (47, 48) (see also Fig. S4 to S9 in the supplemental material) and with the predominance of certain OTUs in amplicon libraries (Fig. 4). Although soil pH is an important environmental parameter impairing activity and community structure of microorganisms, adaption of denitrifier communities to low pH is a common feature of acidic peat denitrifier communities, which are not well represented in denitrifiers of culture collections to date.

Permafrost environments and N_2O fluxes. Even though evidence is accumulating that permafrost-affected systems may play an important role for N-cycling and global N_2O fluxes, many details are still unresolved (45, 47, 58). Further in-depth studies on denitrification and denitrifier communities in permafrost-affected systems are thus needed to reach a higher level of understanding of the possible source and sink functions for N_2O in permafrost peatlands. DNA-based denitrifier community analyses reflect long-term impact of environmental conditions and do not allow for conclusions on the active fraction of the community at a given time point (i.e., resting and dormant cells are included in such analyses). Detection of new organisms via PCR-based structural gene analyses is particularly limited by the selectivity of primers utilized, further complicating matters (25, 35, 68). Thus, transcriptomic and gene expression-based approaches in the future are needed to identify links between active members of the

denitrifier community and observed differences in N_2O fluxes from permafrost peatlands in future studies.

ACKNOWLEDGMENTS

Support for this work was provided by LAPBIAT (part of the Sixth EU Framework Programme Infrastructures), the German Academic Exchange Service (DAAD), the Deutsche Forschungsgemeinschaft (DFG HO 4020/2-2), and the University of Bayreuth.

We are thankful to Jyrki Manninen for organizational help, the team at Kevo research station for excellent support, Christian Hofmann for assistance with gas measurements, the Central Analytics Department of BayCEER for analyses of nitrate, nitrite, ammonium, total carbon, total nitrogen, and total organic carbon, Rolf Daniel and Andrea Thürmer for pyrosequencing, and Steffen Kolb, Markus Nebel, Sebastian Wild, Justin Kuczynski, and Christopher Quince for help with sequence analyses.

REFERENCES

1. **Altschul SF, Gish W, Miller W, Myers EW, Lipman DJ.** 1990. Basic local alignment search tool. J. Mol. Biol. **215**:403–410.
2. **Anisimov, OA.** 2007. Potential feedback of thawing permafrost to the global climate system through methane emission. Environ. Res. Lett. **2**:045016. doi:10.1088/1748–9326/2/4/045016.
3. **Barta J, Melichova T, Vanek D, Picek T, Santruckova H.** 2010. Effect of pH and dissolved organic matter on the abundance of *nirK* and *nirS* denitrifiers in spruce forest soil. Biogeochemistry **101**:123–132.
4. **Bergaust L, Mao YJ, Bakken LR, Frostegård Å.** 2010. Denitrification response patterns during the transition to anoxic respiration and posttranscriptional effects of suboptimal pH on nitrogen oxide reductase in *Paracoccus denitrificans.* Appl. Environ. Microbiol. **76**:6387–6396.
5. **Berry D, Mahfoudh KB, Wagner M, Loy A.** 2011. Barcoded primers used in multiplex amplicon pyrosequencing bias amplification. Appl. Environ. Microbiol. **77**:7846–7849.
6. **Braker G, Conrad R.** 2011. Diversity, structure, and size of N_2O-producing microbial communities in soils—what matters for their functioning? Adv. Appl. Microbiol. **75**:33–70.
7. **Braker G, Dörsch P, Bakken LR.** 2012. Genetic characterization of denitrifier communities with contrasting intrinsic functional traits. FEMS Microbiol. Ecol. **79**:542–554.
8. **Bremner JM.** 1997. Sources of nitrous oxide in soils. Nutr. Cycl. Agroecosys. **49**:7–16.
9. **Bru D, et al.** 2011. Determinants of the distribution of nitrogen-cycling microbial communities at the landscape scale. ISME J. **5**:532–542.
10. **Caporaso JG, et al.** 2010. QIIME allows analysis of high-throughput community sequencing data. Nat. Methods **7**:335–336.
11. **Chapuis-Lardy L, Wrage N, Metay A, Chotte JL, Bernoux M.** 2007. Soils, a sink for N_2O? Global Change Biol. **13**:1–17.
12. **Christensen TR, Michelsen A, Jonasson S.** 1999. Exchange of CH_4 and N_2O in a subarctic heath soil: effects of inorganic N and P and amino acid addition. Soil Biol. Biochem. **31**:637–641.
13. **Conrad R.** 1996. Soil microorganisms as controllers of atmospheric trace gases (H_2, CO, CH_4, OCS, N_2O, and NO). Microbiol. Rev. **60**:609–640.
14. **Cuhel J, et al.** 2010. Insights into the effect of soil pH on N_2O and N_2 emissions and denitrifier community size and activity. Appl. Environ. Microbiol. **76**:1870–1878.
15. **Dandie CE, et al.** 2011. Abundance, diversity and functional gene expression of denitrifier communities in adjacent riparian and agricultural zones. FEMS Microbiol. Ecol. **77**:69–82.
16. **Dörsch P, Braker G, Bakken L.** 2012. Community specific pH response of denitrification: experiments with cells extracted from organic soils. FEMS Microbiol. Ecol. **79**:530–541.
17. **Elberling B, Christiansen HH, Hansen BU.** 2010. High nitrous oxide production from thawing permafrost. Nat. Geosci. **3**:332–335.
18. **Enwall K, Throbäck IN, Stenberg M, Soderstrom M, Hallin S.** 2010. Soil resources influence spatial patterns of denitrifying communities at scales compatible with land management. Appl. Environ. Microbiol. **76**:2243–2250.
19. **Fierer N, Jackson RB.** 2006. The diversity and biogeography of soil bacterial communities. Proc. Natl. Acad. Sci. U. S. A. **103**:626–631.
20. **Forster P, et al.** 2007. Changes in atmospheric constituents and in radiative forcing, p 129–234. *In* Solomon S, et al (ed), Climate change 2007: the physical science basis. Contribution of Working Group I to the Fourth Assessment Report of the Intergovernmental Panel on Climate Change. Cambridge University Press, Cambridge, United Kingdom.
21. **Fronzek S, Carter TR, Raisanen J, Ruokolainen L, Luoto M.** 2010. Applying probabilistic projections of climate change with impact models: a case study for sub-arctic palsa mires in Fennoscandia. Clim. Change **99**:515–534.
22. **Garcia-Lledo A, Vilar-Sanz A, Trias R, Hallin S, Baneras L.** 2011. Genetic potential for N_2O emissions from the sediment of a free water surface constructed wetland. Water Res. **45**:5621–5632.
23. **Goldberg SD, Knorr KH, Blodau C, Lischeid G, Gebauer G.** 2010. Impact of altering the water table height of an acidic fen on N_2O and NO fluxes and soil concentrations. Global Change Biol. **16**:220–233.
24. **Goldberg SD, Knorr KH, Gebauer G.** 2008. N_2O concentration and isotope signature along profiles provide deeper insight into the fate of N_2O in soils. Isotopes Environ. Health Stud. **44**:377–391.
25. **Green SJ, et al.** 2010. Denitrifying bacteria isolated from terrestrial subsurface sediments exposed to mixed-waste contamination. Appl. Environ. Microbiol. **76**:3244–3254.
26. **Green SJ, et al.** 2012. Denitrifying bacteria from the genus *Rhodanobacter* dominate bacterial communities in the highly contaminated subsurface of a nuclear legacy waste site. Appl. Environ. Microbiol. **78**:1039–1047.
27. **Hallin S, Jones CM, Schloter M, Philippot L.** 2009. Relationship between N-cycling communities and ecosystem functioning in a 50-year-old fertilization experiment. ISME J. **3**:597–605.
28. **Henry S, Bru D, Stres B, Hallet S, Philippot L.** 2006. Quantitative detection of the *nosZ* gene, encoding nitrous oxide reductase, and comparison of the abundances of 16S rRNA, *narG*, *nirK*, and *nosZ* genes in soils. Appl. Environ. Microbiol. **72**:5181–5189.
29. **Heylen K, et al.** 2006. The incidence of *nirS* and *nirK* and their genetic heterogeneity in cultivated denitrifiers. Environ. Microbiol. **8**:2012–2021.
30. **Holtan-Hartwig L, Dörsch P, Bakken LR.** 2000. Comparison of denitrifying communities in organic soils: kinetics of NO_3^- and N_2O reduction. Soil Biol. Biochem. **32**:833–843.
31. **Horn MA, Matthies C, Küsel K, Schramm A, Drake HL.** 2003. Hydrogenotrophic methanogenesis by moderately acid-tolerant methanogens of a methane-emitting acidic peat. Appl. Environ. Microbiol. **69**:74–83.
32. **Huang S, Chen C, Yang X, Wu Q, Zhang R.** 2011. Distribution of typical denitrifying functional genes and diversity of the *nirS*-encoding bacterial community related to environmental characteristics of river sediments. Biogeosciences **8**:3041–3051.
33. **Huse SM, Welch DM, Morrison HG, Sogin ML.** 2010. Ironing out the wrinkles in the rare biosphere through improved OTU clustering. Environ. Microbiol. **12**:1889–1898.
34. **Ishii S, Ohno H, Tsuboi M, Otsuka S, Senoo K.** 2011. Identification and isolation of active N_2O reducers in rice paddy soil. ISME J. **5**:1936–1945.
35. **Jones CM, Stres B, Rosenquist M, Hallin S.** 2008. Phylogenetic analysis of nitrite, nitric oxide, and nitrous oxide respiratory enzymes reveal a complex evolutionary history for denitrification. Mol. Biol. Evol. **25**:1955–1966.
36. **Jones CM, et al.** 2011. Phenotypic and genotypic heterogeneity among closely related soil-borne N_2- and N_2O-producing *Bacillus* isolates harboring the *nosZ* gene. FEMS Microbiol. Ecol. **76**:541–552.
37. **Keil D, et al.** 2011. Influence of land-use intensity on the spatial distribution of N-cycling microorganisms in grassland soils. FEMS Microbiol. Ecol. **77**:95–106.
38. **Klemedtsson L, von Arnold K, Weslien P, Gundersen P.** 2005. Soil CN ratio as a scalar parameter to predict nitrous oxide emissions. Global Change Biol. **11**:1142–1147.
39. **Kolb S, Horn MA.** 2012. Microbial CH_4 and N_2O consumption in acidic wetlands. Front. Microbiol. **3**:78. doi:10.3389/fmicb. 2012.00078.
40. **Kumar S, Nei M, Dudley J, Tamura K.** 2008. MEGA: A biologist-centric software for evolutionary analysis of DNA and protein sequences. Brief. Bioinform. **9**:299306. doi:10.1093/bib/bbn017.
41. **Kunin V, Engelbrektson A, Ochman H, Hugenholtz P.** 2010. Wrinkles in the rare biosphere: pyrosequencing errors can lead to artificial inflation of diversity estimates. Environ. Microbiol. **12**:118–123.
42. **Lauber CL, Hamady M, Knight R, Fierer N.** 2009. Pyrosequencing-based assessment of soil pH as a predictor of soil bacterial community structure at the continental scale. Appl. Environ. Microbiol. **75**:5111–5120.
43. **Liu BB, Mørkved PT, Frostegård Å, Bakken LR.** 2010. Denitrification

gene pools, transcription and kinetics of NO, N_2O and N_2 production as affected by soil pH. FEMS Microbiol. Ecol. **72**:407–417.
44. **Martikainen PJ, Nykänen H, Crill P, Silvola J.** 1993. Effect of a lowered water-table on nitrous-oxide fluxes from northern peatlands. Nature **366**: 51–53. (Letter.)
45. **Marushchak ME, et al.** 2011. Hot-spots for nitrous oxide emissions found in different types of permafrost peatlands. Global Change Biol. **17**:2601–2614.
46. **Nebel ME, et al.** 2011. JAguc—a software package for environmental diversity analyses. J. Bioinform. Comput. Biol. **9**:749–773.
47. **Palmer K, Biasi C, Horn MA.** 2012. Contrasting denitrifier communities relate to contrasting N_2O emission patterns from acidic peat soils in arctic tundra. ISME J. **6**:1058–1077.
48. **Palmer K, Drake HL, Horn MA.** 2010. Association of novel and highly diverse acid-tolerant denitrifiers with N_2O fluxes of an acidic fen. Appl. Environ. Microbiol. **76**:1125–1134.
49. **Palmer K, Drake HL, Horn MA.** 2009. Genome-derived criteria for assigning environmental *narG* and *nosZ* sequences to operational taxonomic units of nitrate reducers. Appl. Environ. Microbiol. **75**:5170–5174.
50. **Parkin TB, Sexstone AJ, Tiedje JM.** 1985. Adaptation of denitrifying populations to low soil-pH. Appl. Environ. Microbiol. **49**:1053–1056.
51. **Philippot L, et al.** 2009. Mapping field-scale spatial patterns of size and activity of the denitrifier community. Environ. Microbiol. **11**:1518–1526.
52. **Philippot L, Hojberg O.** 1999. Dissimilatory nitrate reductases in bacteria. Biochim. Biophys. Acta **1446**:1–23.
53. **Philippot L, Piutti S, Martin-Laurent F, Hallet S, Germon JC.** 2002. Molecular analysis of the nitrate-reducing community from unplanted and maize-planted soils. Appl. Environ. Microbiol. **68**:6121–6128.
54. **Post WM, Pastor J, Zinke PJ, Stangenberger AG.** 1985. Global patterns of soil-nitrogen storage. Nature **317**:613–616. (Letter.)
55. **Prakash O, et al.** 25 November 2011, posting date. Description of *Rhodanobacter denitrificans* sp. nov., isolated from nitrate-rich zones of a contaminated aquifer. Int. J. Syst. Evol. Microbiol. doi:10.1099/ijs.0.035840-0.
56. **Quince C, Lanzen A, Davenport RJ, Turnbaugh PJ.** 2011. Removing noise from pyrosequenced amplicons. BMC Bioinformatics **12**:38. doi:10.1186/1471-2105-12-38.
57. **Ravishankara AR, Daniel JS, Portmann RW.** 2009. Nitrous oxide (N_2O): the dominant ozone-depleting substance emitted in the 21st century. Science **326**:123–125.
58. **Repo ME, et al.** 2009. Large N_2O emissions from cryoturbated peat soil in tundra. Nat. Geosci. **2**:189–192.
59. **Rich JJ, Heichen RS, Bottomley PJ, Cromack K, Myrold DD.** 2003. Community composition and functioning of denitrifying bacteria from adjacent meadow and forest soils. Appl. Environ. Microbiol. **69**:5974–5982.
60. **Saitou N, Nei M.** 1987. The neighbor-joining method—a new method for reconstructing phylogenetic trees. Mol. Biol. Evol. **4**:406–425.
61. **Segel IH.** 1993. Enzyme kinetics: behavior and analysis of rapid equilibrium and steady-state enzyme systems. John Wiley & Sons, New York, NY.
62. **Seppälä M.** 1988. Palsas and related forms, p 247–278. *In* Clark MJ (ed), Advances in periglacial geomorphology. Wiley, Chichester, United Kingdom.
63. **Seppälä M.** 2011. Synthesis of studies of palsa formation underlining the importance of local environmental and physical characteristics. Quat. Res. **75**:366–370.
64. **Šimek M, Cooper JE.** 2002. The influence of soil pH on denitrification: progress towards the understanding of this interaction over the last 50 years. Eur. J. Soil. Sci. **53**:345–354.
65. **Steven B, Pollard WH, Greer CW, Whyte LG.** 2008. Microbial diversity and activity through a permafrost/ground ice core profile from the Canadian high Arctic. Environ. Microbiol. **10**:3388–3403.
66. **Takakai F, et al.** 2008. CH_4 and N_2O emissions from a forest-alas ecosystem in the permafrost taiga forest region, eastern Siberia, Russia. J. Geophys. Res. Biogeosci. **113**:G02002. doi:10.1029/2007JG000521.
67. **Tarnocai C, et al.** 2009. Soil organic carbon pools in the northern circumpolar permafrost region. Global Biogeochem. Cycles **23**:GB2023. doi:10.1029/2008GB003327.
68. **Throbäck IN, Enwall K, Jarvis A, Hallin S.** 2004. Reassessing PCR primers targeting *nirS*, *nirK* and *nosZ* genes for community surveys of denitrifying bacteria with DGGE. FEMS Microbiol. Ecol. **49**:401–417.
69. **van Cleemput O.** 1998. Subsoils: chemo- and biological denitrification, N_2O and N_2 emissions. Nutr. Cycling Agroecosyst. **52**:187–194.
70. **van den Heuvel RN, van der Biezen E, Jetten MSM, Hefting MM, Kartal B.** 2010. Denitrification at pH 4 by a soil-derived *Rhodanobacter*-dominated community. Environ. Microbiol. **12**:3264–3271.
71. **Werner C, Butterbach-Bahl K, Haas E, Hickler T, Kiese R.** 2007. A global inventory of N_2O emissions from tropical rainforest soils using a detailed biogeochemical model. Global Biogeochem. Cycles **21**:GB3010. doi:10.1029/2006GB002909.
72. **Yoshinari T, Knowles R.** 1976. Acetylene inhibition of nitrous oxide reduction by denitrifying bacteria. Biochem. Biophys. Res. Commun. **69**: 705–710.
73. **Zaprasis A, Liu YJ, Liu SJ, Drake HL, Horn MA.** 2010. Abundance of novel and diverse *tfdA*-like genes, encoding putative phenoxyalkanoic acid herbicide-degrading dioxygenases, in soil. Appl. Environ. Microbiol. **76**:119–128.
74. **Zhou JZ, et al.** 2011. Reproducibility and quantitation of amplicon sequencing-based detection. ISME J. **5**:1303–1313.
75. **Zoltai SC.** 1972. Palsas and peat plateaus in central Manitoba and Saskatchewan. Can. J. Forestry Res. **2**:291–302.
76. **Zumft WG.** 1997. Cell biology and molecular basis of denitrification. Microbiol. Mol. Biol. Rev. **61**:533–615.
77. **Zumft WG.** 2005. Nitric oxide reductases of prokaryotes with emphasis on the respiratory, heme-copper oxidase type. J. Inorg. Biochem. **99**:194–215.
78. **Zumft WG, Kroneck PM.** 2007. Respiratory transformation of nitrous oxide (N_2O) to dinitrogen by Bacteria and Archaea. Adv. Microb. Physiol. **52**:107–227.